

LA-UR-14-21259

Approved for public release; distribution is unlimited.

Title: Applying Nonlinear Diffusion Acceleration to Fixed-Source Problems with Anisotropic Scattering

Author(s): Willert, Jeffrey A.
Park, Hyeongkae
Taitano, William

Intended for: 18th Topical Meeting of the Radiation Shielding & Protection Division of American Nuclear Society, 2014-09-14 (Knoxville, Tennessee, United States)

Issued: 2014-02-27



Disclaimer:

Los Alamos National Laboratory, an affirmative action/equal opportunity employer, is operated by the Los Alamos National Security, LLC for the National Nuclear Security Administration of the U.S. Department of Energy under contract DE-AC52-06NA25396. By approving this article, the publisher recognizes that the U.S. Government retains nonexclusive, royalty-free license to publish or reproduce the published form of this contribution, or to allow others to do so, for U.S. Government purposes. Los Alamos National Laboratory requests that the publisher identify this article as work performed under the auspices of the U.S. Department of Energy. Los Alamos National Laboratory strongly supports academic freedom and a researcher's right to publish; as an institution, however, the Laboratory does not endorse the viewpoint of a publication or guarantee its technical correctness.

Applying Nonlinear Diffusion Acceleration to Fixed-Source Problems with Anisotropic Scattering

Jeffrey Willert, H. Park, William Taitano

Theoretical Division, MS B216, Los Alamos National Laboratory, Los Alamos, NM 87545
jaw@lanl.gov, hkpark@lanl.gov, taitano@lanl.gov

INTRODUCTION

Work over the last several years has demonstrated the impressive performance gains that can be attained by using Moment-Based Acceleration (MBA), or High-Order/Low-Order (HOLO), methods in a variety of transport applications [2, 7, 5, 4]. In the field of neutronics, Nonlinear Diffusion Acceleration (NDA) [1, 2, 7] has been used to accelerate the solution to the fixed-source problem and the k -eigenvalue problem. These methods efficiently move a major portion of the computational work out of the full phase-space (high-order (HO)) domain into a reduced phase-space (low-order (LO)) setting. In previous implementations, NDA has only been applied to isotropic scattering problems. In this paper, we will extend this methodology to anisotropic scattering.

This initial work on anisotropic scattering will focus on the 1-D multi-group neutron transport equation,

$$\mu \frac{\partial \psi^g}{\partial x} + \Sigma_t^g \psi^g = \frac{1}{2} \left[\sum_{g'=1}^G \sum_{l=0}^L (2l+1) P_l(\mu) \Sigma_{s,l}^{g' \rightarrow g} \phi_l^{g'} \right] + \frac{1}{2} Q^g, \quad (1)$$

in which ψ^g is the g^{th} group angular flux, Q^g is an isotropic source, and ϕ_l^g is the l^{th} Legendre moment of ψ^g . That is

$$\phi_l^g = \int_{-1}^1 P_l(\mu) \psi^g(x, \mu) d\mu, \quad (2)$$

where $P_l(\mu)$ is the l^{th} Legendre polynomial [3]. $\phi \equiv \phi_0 = \int \psi d\mu$ is known as the scalar flux and $J \equiv \phi_1 = \int \mu \psi d\mu$ will be referred to as the current. Additionally, Σ_t and Σ_s are the total and scattering cross-sections, respectively. This summary focuses on a fixed-source problem, but the extension to criticality problems is straight-forward via NDA-NCA as in [7].

LOW ORDER SYSTEM

Given the transport equation

$$\mu \frac{\partial \psi^g}{\partial x} + \Sigma_t^g \psi^g = \frac{1}{2} \left[\sum_{g'=1}^G \sum_{l=0}^L (2l+1) P_l(\mu) \Sigma_{s,l}^{g' \rightarrow g} \phi_l^{g'} \right] + \frac{1}{2} Q^g, \quad (3)$$

let us compute the 0th and 1st angular moments:

$$\frac{dJ^g}{dx} + \Sigma_t^g \phi^g = \sum_{g'=1}^G \Sigma_{s,0}^{g' \rightarrow g} \phi^{g'} + Q^g \quad (4)$$

$$\frac{dE^g \phi^g}{dx} + \Sigma_t^g J^g = \sum_{g'=1}^G \Sigma_{s,1}^{g' \rightarrow g} J^{g'}, \quad (5)$$

in which E is the Eddington tensor.

For isotropic scattering, NDA was originally formulated to replace the current, J^g , by

$$J^g = -\frac{1}{3\Sigma_t^g} \frac{d\phi^g}{dx} + \hat{D}^g \phi^g \quad (6)$$

in the zeroth moment equation [2]. In Equation 6, \hat{D} is commonly referred to as the “consistency term,” as it provides discrete consistency between the HO and the LO system. However, the extra terms from the anisotropic scattering sources in Equation 5 require more intricate care. Now, each of the group first moment equations are coupled via the group-to-group anisotropic scattering source.

Let us rewrite each of the first moment equations by replacing the Eddington tensor with $\frac{1}{3}$ and add in a correction term to account for the Eddington tensor approximation,

$$\frac{1}{3} \frac{d\phi^g}{dx} + \Sigma_t^g J^g = \sum_{g'=1}^G \Sigma_{s,1}^{g' \rightarrow g} J^{g'} + \Sigma_{tr}^g \hat{D}^g \phi^g, \quad (7)$$

where

$$\Sigma_{tr}^g = \Sigma_t^g - \Sigma_{s,1}^g. \quad (8)$$

We can evaluate \hat{D} by replacing ϕ and J with high-order quantities. That is, we replace ϕ and J by moments of the angular flux and rearrange the equation for \hat{D} ,

$$\frac{\frac{1}{3} \frac{d\phi^g}{dx} + \Sigma_t^g J^g - \sum_{g'=1}^G \Sigma_{s,1}^{g' \rightarrow g} J^{g'}}{\Sigma_{tr}^g \phi^g} = \hat{D}^g. \quad (9)$$

We can write this in a slightly more familiar form by pulling the in-group anisotropic scattering term out of the sum,

$$\frac{\frac{1}{3\Sigma_{tr}^g} \frac{d\phi^g}{dx} + J^g - \frac{1}{\Sigma_{tr}^g} \sum_{g' \neq g} \Sigma_{s,1}^{g' \rightarrow g} J^{g'}}{\phi^g} = \hat{D}^g. \quad (10)$$

Solving for J^g to obtain a closure as we did in Equation 4 requires the solution to a $G \times G$ matrix equation at each cell face:

$$\begin{pmatrix} \Sigma_{tr}^1 & -\Sigma_{s,1}^{2 \rightarrow 1} & \dots & -\Sigma_{s,1}^{G \rightarrow 1} \\ -\Sigma_{s,1}^{1 \rightarrow 2} & \Sigma_{tr}^2 & \dots & -\Sigma_{s,1}^{G \rightarrow 2} \\ \vdots & \vdots & \ddots & \vdots \\ -\Sigma_{s,1}^{1 \rightarrow G} & -\Sigma_{s,1}^{2 \rightarrow G} & \dots & \Sigma_{tr}^G \end{pmatrix} \begin{pmatrix} J^1 \\ J^2 \\ \vdots \\ J^G \end{pmatrix} = \quad (11)$$

$$\begin{pmatrix} -\frac{1}{3} \frac{d\phi^1}{dx} + \Sigma_{tr}^1 \hat{D}^1 \phi^1 \\ -\frac{1}{3} \frac{d\phi^2}{dx} + \Sigma_{tr}^2 \hat{D}^2 \phi^2 \\ \vdots \\ -\frac{1}{3} \frac{d\phi^G}{dx} + \Sigma_{tr}^G \hat{D}^G \phi^G \end{pmatrix}. \quad (12)$$

2-Group Anisotropic Problem

In order to develop a working example, let us consider the case in which $G = 2$ and there is no upscattering from the thermal to the fast group. Now, $\Sigma_{s,1}^{2 \rightarrow 1} = 0$ and our system of equations reduces to

$$\begin{pmatrix} \Sigma_{tr}^1 & 0 \\ -\Sigma_{s,1}^{1 \rightarrow 2} & \Sigma_{tr}^2 \end{pmatrix} \begin{pmatrix} J^1 \\ J^2 \end{pmatrix} = \begin{pmatrix} -\frac{1}{3} \frac{d\phi^1}{dx} + \Sigma_{tr}^1 \hat{D}^1 \phi^1 \\ -\frac{1}{3} \frac{d\phi^2}{dx} + \Sigma_{tr}^2 \hat{D}^2 \phi^2 \end{pmatrix}. \quad (13)$$

This triangular system is easily solved by forward substitution,

$$J^1 = -\frac{1}{3\Sigma_{tr}^1} \frac{d\phi^1}{dx} + \hat{D}^1 \phi^1 \quad (14)$$

$$J^2 = \frac{\Sigma_{s,1}^{1 \rightarrow 2}}{\Sigma_{tr}^2} \left(-\frac{1}{3\Sigma_{tr}^1} \frac{d\phi^1}{dx} + \hat{D}^1 \phi^1 \right) - \frac{1}{3\Sigma_{tr}^2} \frac{d\phi^2}{dx} + \hat{D}^2 \phi^2. \quad (15)$$

This closure relationship is very familiar – the only difference is that a scaled copy of J^1 must be included in the definition of J^2 . This yields an interesting low-order system

$$\frac{d}{dx} \left[-\frac{1}{3\Sigma_{tr}^1} \frac{d\phi^1}{dx} + \hat{D}^1 \phi^1 \right] + \Sigma_a^1 \phi^1 = Q^1 \quad (16)$$

$$\frac{d}{dx} \left[\frac{\Sigma_{s,1}^{1 \rightarrow 2}}{\Sigma_{tr}^2} \left(-\frac{1}{3\Sigma_{tr}^1} \frac{d\phi^1}{dx} + \hat{D}^1 \phi^1 \right) - \frac{1}{3\Sigma_{tr}^2} \frac{d\phi^2}{dx} + \hat{D}^2 \phi^2 \right] + \Sigma_a^2 \phi^2 = \Sigma_{s,0}^{1 \rightarrow 2} \phi^1 + Q^2 \quad (17)$$

We see that in the low-order system there is an additional coupling between groups caused by the linearly anisotropic down-scattering. This system is still sparse and block lower-triangular. It is important to note that this low-order system is consistent, regardless of the degrees of anisotropy in the scattering.

NDA FOR ANISOTROPIC FIXED-SOURCE PROBLEMS

The most basic method for solving the fixed-source neutron transport problem is known as *source iteration* [3]. Source iteration utilizes successive substitution to yield a sequence of Legendre moments of the angular flux,

$$\mu \frac{\partial \psi^{g,k+1}}{\partial x} + \Sigma_t^g \psi^{g,k+1} = \frac{1}{2} \left[\sum_{g'=1}^G \sum_{l=0}^L (2l+1) P_l(\mu) \Sigma_{s,l}^{g' \rightarrow g} \phi_l^{g',k} \right] + \frac{1}{2} Q^g, \quad (18)$$

$$\phi_l^{g',k+1} = \int P_l(\mu) \psi^{g,k+1} d\mu. \quad (19)$$

This iteration may converge arbitrarily slowly when the domain is large (in terms of mean-free-paths) and the scattering ratio, Σ_s/Σ_t , is close to one [3]. This fact makes source iteration a poor choice for large computations. For this reason, we choose to utilize NDA to accelerate the scattering source, similar to the work that was done in [1, 3].

The Picard-NDA algorithm inserts a low-order solve after each transport sweep to accelerate the convergence of the P_0 and P_1 scattering sources. This algorithm is formally described in Algorithm 1.

Algorithm 1 Picard NDA

Picard NDA

Input Φ^0 , tolerance.

$k = 0$.

while $\frac{\|\phi^{g,k+1} - \phi^{g,k}\|}{\|\phi^{g,k+1}\|} > \text{tolerance}$ for any g **do**

Execute a transport sweep to recover the angular flux

$$\mu \frac{\partial \psi^{g,HO}}{\partial x} + \Sigma_t^g \psi^{g,HO} = \frac{1}{2} \left[\sum_{g'=1}^G \sum_{l=0}^L (2l+1) P_l(\mu) \Sigma_{s,l}^{g' \rightarrow g} \phi_l^{g',k} \right] + \frac{1}{2} Q^g, \quad (20)$$

Compute high-order moments

$$\phi^{g,HO} = \int_{-1}^1 \psi^{g,HO} d\mu \quad (21)$$

$$J^{g,HO} = \int_{-1}^1 \mu \psi^{g,HO} d\mu. \quad (22)$$

Compute \hat{D}^g for each group

$$\frac{\frac{1}{3\Sigma_{tr}^g} \frac{d\phi^{g,HO}}{dx} + J^{g,HO} - \frac{1}{\Sigma_{tr}^g} \sum_{g' \neq g} \Sigma_{s,1}^{g' \rightarrow g} J^{g',HO}}{\phi^{g,HO}} = \hat{D}^g. \quad (23)$$

Solve the low-order system for new ϕ and J

$$\frac{dJ^{g,k+1}}{dx} + \Sigma_t^g \phi^{g,k+1} = \sum_{g'=1}^G \Sigma_{s,0}^{g' \rightarrow g} \phi^{g',k+1} + Q^g \quad (24)$$

$$\frac{1}{3} \frac{d\phi^{g,k+1}}{dx} + \Sigma_t^g J^{g,k+1} = \sum_{g'=1}^G \Sigma_{s,1}^{g' \rightarrow g} J^{g',k+1} + \Sigma_{tr}^g \hat{D}^g \phi^{g,k+1}. \quad (25)$$

Compute $l \geq 2$ Legendre moments

$$\phi_l^{g,k+1} = \int P_l(\mu) \psi^{g,HO} d\mu. \quad (26)$$

Increment $k = k + 1$.

end while

As one can see in Algorithm 1, the low-order system provides the P_0 and P_1 scattering moments (ϕ and J) for the subsequent transport sweep. In this sense, both ϕ and J are “accelerated” by the low-order system, while higher-order Legendre moments $l \geq 2$ are left unaccelerated. For the problems we are interested in, the isotropic and linear anisotropic scattering sources make up the greatest contribution to the scattering source and are the slowest scattering moments to converge. For problems in which the higher-order Legendre moments comprise a major portion of the scattering source, the Picard NDA algorithm may be less effective. These higher-order moments could be accelerated by incorporating more angular moments in the low-order system. We will demonstrate the impressive performance of this algorithm in the following section.

NUMERICAL RESULTS

In this section we will test these algorithms on three 1-D fixed-source problems. For each of the following tests we use an S_{32} angular quadrature and a diamond-difference spatial discretization [3]. We will use a convergence tolerance of 10^{-8} for each test, where the metric of convergence is a relative change in each Legendre moment from iteration m to $m + 1$.

For each test, we plot the relative difference of each Legendre moment compared at successive iterations. That is, we plot,

$$\frac{\|\phi_l^m - \phi_l^{m-1}\|}{\|\phi_l^m\|} \quad (27)$$

for each l .

Results: Fixed-Source Test Problem: Test 1

In this section we will consider a single-group, anisotropic scattering fixed-source problem which we design to be challenging (in terms of number of transport sweeps) for the source iteration algorithm. The material properties are described in Table I. The anisotropic cross-sections are given in the table for $l = 1, 2, 3$. $\Sigma_{s,l} = 0$ for $l > 3$. We use 2000 spatial cells for this problem.

TABLE I. Material Properties: 1-D Fixed-Source

Property	Mat. 1	Mat. 2	Mat. 3	Mat. 4	Mat. 5
x - range	[0, 10]	[10, 90]	[90, 110]	[110, 190]	[190, 200]
Σ_t	1.000	1.000	1.000	1.000	1.000
$\Sigma_{s,0}$	0.500	0.999	0.500	0.999	0.500
$\Sigma_{s,l}$	0.100	0.100	0.100	0.100	0.100
$Q(x)$	0.000	0.500	0.000	0.500	0.000

A plot of the convergence of each Legendre moment of the angular flux is presented in Figure 1. As one can see from the plot, when source iteration is used, over 7700 transport sweeps are required to converge each of the Legendre moments to a tolerance of 10^{-8} . Compare this to the mere 16 sweeps required by NDA. Looking closely at the plot, one can see that when source iteration is used, the scalar flux and current (P_0 and P_1 , respectively) are the slowest to converge. Contrast this with NDA, in which the flux and current converge more rapidly than the higher order Legendre moments. This is precisely the goal of NDA - accelerate the convergence of the scalar flux and current.

Results: Fixed-Source Test Problem: 2-Group Test

In this section we will consider a two-group, anisotropic scattering fixed-source problem which we have adapted from [9]. The material properties are described in Table II. We use 1000 spatial cells for this problem.

In Figure 2, we see the same behavior as was demonstrated in the single-group test. NDA provides roughly a 22x speedup over SI. This demonstrates that NDA can easily be applied

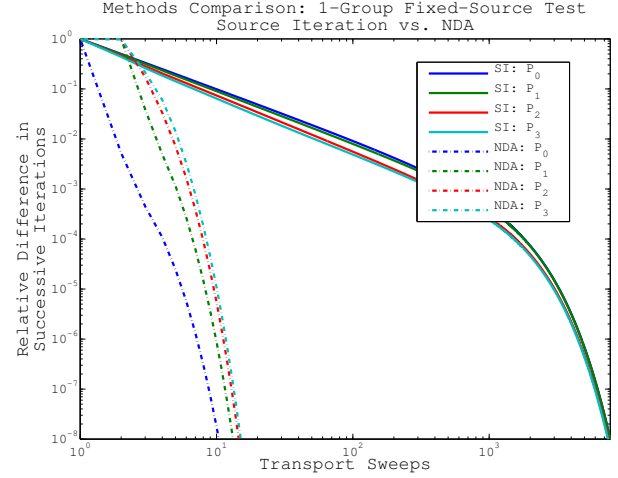


Fig. 1. Convergence plot for 1-D, 1 group, anisotropic, fixed-source test.

TABLE II. Material Properties: 1-D 2-Group Fixed-Source

Property	Material 1	
x - range (cm)	[0, 130]	
Group	1	2
Σ_t^g	0.656960	2.5202500
$\Sigma_{s,0}^{1 \rightarrow g}$	0.6256800	0.0292270
$\Sigma_{s,0}^{2 \rightarrow g}$	0.0000000	2.4438300
$\Sigma_{s,1}^{1 \rightarrow g}$	0.2745900	0.0075737
$\Sigma_{s,1}^{2 \rightarrow g}$	0.0000000	0.8331800

to multigroup problems, additionally. Each of the Legendre moments smoothly and quickly converges to zero when NDA is applied.

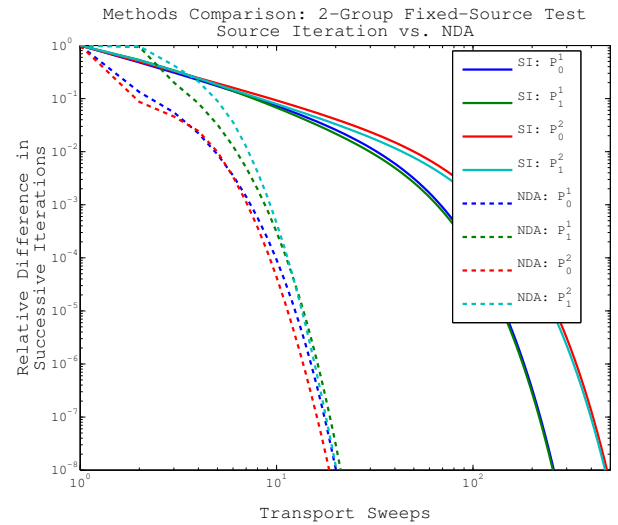


Fig. 2. Convergence plot for 1-D, 1 group, anisotropic, fixed-source test.

Results: Fixed-Source Test Problem: Henyey-Greenstein

For the third set of test problems we will use the Henyey-Greenstein function [8] to generate forward-peaked scattering cross-sections. In 1-D, this function is given by

$$p(\mu) = \frac{1}{2} \frac{1 - h^2}{(1 + h^2 - 2h\mu)^{\frac{3}{2}}} \quad (28)$$

$$= \sum_{l=0}^{\infty} (2l+1)h^l P_l(\mu) \quad (29)$$

in which h is a parameter that measures the “forward-peakedness” of the scattering operator and $P_l(\mu)$ is again the l^{th} Legendre polynomial. We generally truncate the series at some L . When h is near zero, scattering is approximately isotropic, so we would expect NDA to perform well. However, as h increases, we expect the performance to degrade, while still offering some acceleration. We will solve the problem for $L = 5$ for a series of h for the configuration described in Table III.

TABLE III. Material Properties: Henyey-Greenstein

Property	Mat. 1	Mat. 2
x - range	[0, 1]	[9, 10]
Σ_t	1.000	1.000
$\Sigma_{s,0}$	0.990	0.990
$Q(x)$	0.500	0.000

In Table IV we present the total number of transport sweeps to converge each of the six Legendre moments of the angular flux to the desired tolerance.

TABLE IV. Total Iterations: Henyey-Greenstein

h	0.000	0.125	0.250	0.375
NDA	14	21	49	162
SI	701	594	415	583

As we can see, NDA provides a significant acceleration over SI for each h tested. This acceleration is most prominent when $h \approx 0$, and becomes less impressive as h increases. Even at $h = .375$, NDA provides a 3.5x speed-up over SI. For the isotropic problem NDA provides a 50x speed-up.

CONCLUSIONS

Within this paper, we have described a method for extending Nonlinear Diffusion Acceleration to solve problems with anisotropic scattering. We demonstrated that a consistent low-order system, resembling the low-order system from [2], could be constructed. We demonstrated that the NDA method performed exceptionally in the presence of anisotropic scattering. NDA reduced the number of iterations required to meet the convergence tolerance by a factor of 500 over source iter-

ation for a one fixed-source problem and by 3.5-50x for the Henyey-Greenstein problems.

As mentioned in the introduction, this method is equally well-suited for eigenvalue problems. The NDA method allows us to transition the eigenvalue iteration to the low-order domain, as in [7]. This is currently ongoing research. Further future work will involve accelerating higher-order Legendre moments in addition to the P_0 and P_1 moments. This can be accomplished by incorporating more moments in the LO system or by including some modern nonlinear solver technology.

ACKNOWLEDGMENTS

This work was performed under U.S. government contract DE-AC52-06NA25396 for Los Alamos National Laboratory, which is operated by Los Alamos National Security, LLC, for the U.S. Department of Energy.

REFERENCES

1. K. S. Smith and J. D. Rhodes III, *Full-Core, 2-D, LWR Core Calculations with CASMO-4E*, Proceedings of the International Conference on New Frontiers of Nuclear Technology: Reactor Physics, Safety and High-Performance Computing (PHYSOR 2002), Seoul, Korea, October 7-10, 2002, American Nuclear Society (2002).
2. D.A. Knoll, Kord Smith, and H. Park, *Application of the Jacobian-Free Newton-Krylov method to nonlinear acceleration of transport source iteration in slab geometry*, Nuclear Science and Engineering, 167(2):122-132, 2011.
3. E. E. Lewis and W. F. Miller, *Computational Methods of Neutron Transport*, American Nuclear Society, Inc., La Grange Park, 1993.
4. William T. Taitano, Dana A. Knoll, Luis Chacón, and Guangye Chen, *Development of a Consistent and Stable Fully Implicit Moment Method for Vlasov-Ampère Particle in Cell (PIC) System*, SIAM J. Sci. Comput., 35(5). 126-149, 2013.
5. H. Park, D. A. Knoll, R. M. Rauenzahn, A. B. Wollaber and J. D. Densmore, *A Consistent, Moment-Based, Multi-scale Solution Approach for Thermal Radiative Transfer Problems*, Transport Theory and Statistical Physics, 41:3-4, 284-303, 2012.
6. Avneet Sood, R. Arthur Forster, and D. Kent Parsons, *Analytical Benchmark Test Set For Criticality Code Verification*, Progress in Nuclear Energy, 42(1):55-106, 2003.
7. H. Park, D.A. Knoll, and C.K. Newman, *Nonlinear Acceleration of Transport Criticality Problems*, Nuclear Science and Engineering, 171:1-14, 2012.
8. L. G. Henyey and J. L. Greenstein, *Astrophysical Journal*, 93, 70, 1941.
9. Avneet Sood, R. Arthur Forster, and D. Kent Parsons, *Analytical Benchmark Test Set For Criticality Code Verification*, Progress in Nuclear Energy, 42(1):55-106, 2003.